RESEARCH ARTICLE

A study of bacteria producing carbonic anhydrase enzyme for CaCO$_3$ precipitation and soil biocementation

Wilson Mwandira[1] · Maria Mavroulidou[1] · Martijn Timmermans[2] · Michael John Gunn[1] · Christopher Gray[1] · Leonardo Pantoja-Muñoz[2] · Diane Purchase[2]

Abstract
We study the carbonic anhydrase (CA) pathway using autochthonous CA-producing bacteria as a means of inducing calcite precipitation, which acts as a biocement to improve the engineering soil properties. Forty different microbial strains producing CA were isolated from the foundation soil of a railway embankment in Prickwillow, UK. Three of the best CA-producing strains were selected and identified by DNA sequencing as *Bacillus licheniformis*, *Bacillus toyonensis* and *Bacillus pumilus* with CA activity values respectively of 1.79 U/ml, 1.42 U/ml and 1.55 U/ml. To optimise the treatments, we investigated the effect of pH, temperature, zinc co-factor and cementation solution molarity on the growth and CA activity and bioprecipitates, with CO$_2$ added in the form of bicarbonate. Scanning electron microscope (SEM) analysis of the bioprecipitates showed that these had characteristic morphologies of calcite and vaterite crystals. The formation of calcite was further corroborated by FT-IR and Raman analysis of bioprecipitates. The precultured bacteria were injected into the fine-grained soil together with cementation solution. Unconfined compressive strength in treated soil increased up to 1 MPa, and its calcium carbonate content increased by 2.78%. This, as well as the stability of the treated soil upon water immersion, proved the biocementation of the fine-grained soil. These findings suggest the potential of employing the CA biocementation route for soil stabilisation pending further development of the technique.

Keywords Carbonic anhydrase enzyme · Microbiological study · Calcite precipitation · Biocementation · Ground improvement

Introduction

Population shifts from rural to urban areas are forcing engineers to construct on inferior ground. To enable this, ground improvement has increasingly been used in geotechnical engineering practice (Astaraki and Esmaeili 2022; Safdar et al. 2022). Different ground improvement methods include mechanical, physical and chemical techniques; these methods suffer from several shortcomings
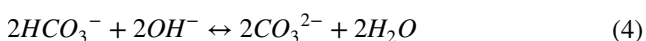

✉ Maria Mavroulidou
  mavroum@lsbu.ac.uk

[1] Division of CIBSE, School of the Built Environment and Architecture, London South Bank University, London, UK

[2] Department of Natural Sciences, Faculty of Science and Technology, Middlesex University, London, UK

linked to costs, heavy machinery and disturbance of services and environmental or human health side effects (Naeimi and Haddad 2020). Chemical ground improvement methods in particular use most commonly lime (Kichou et al. 2022, Zhang et al. 2014 and 2015) and Portland cement (PC) (Lorenzo and Bergado 2006), whose production consumes a high amount of energy and emits 8–10% of global CO$_2$ (Mavroulidou et al. 2022a). Efforts are being made to develop alternative forms of cement for ground improvement, which are ecologically friendlier and require less energy in their manufacture. Examples of such cements include alkali activated/geopolymer cements (e.g. Singhi et al 2017; Coudert et al. 2019; Rios et al 2019; Banaś et al 2020; Mavroulidou et al. 2022b; Mavroulidou et al. 2023) and biocements (e.g. Whiffin 2004; van Paassen et al. 2010; Gomez et al 2017; Chittoori et al. 2018; Mwandira et al. 2019; Mwandira et al. 2021; Lee et al. 2023). Biocements have emerged as a promising environmentally friendly alternative to PC as they are biomimetic

(nature-based). Biocements harness the metabolic action of microorganisms to precipitate biominerals acting as binders of soil particles, which increase soil stiffness and strength. The most commonly precipitated minerals are carbonates, mainly calcium carbonate. The acronym MICP (microbially induced carbonate precipitation) is used to refer to this process, although precipitation of different biominerals (other than carbonates) is possible and has also been studied (e.g. Amarakoon et al. 2014).

Different bacterial species precipitate carbonates in their natural habitats via various metabolic pathways that include ureolysis, denitrification, methane oxidation, photosynthesis, sulfate reduction, iron reduction and the interconversion between CO_2 and the bicarbonate ion HCO_3^- mediated by heterotrophic carbonic anhydrase (CA)–producing bacteria (Mwandira et al 2023b). Of these, the CA pathway is of particular interest, as it can produce biominerals for biocementation via the consumption of CO_2 according to the following chemical reactions: first, CA utilises CO_2, to form hydrated aqueous CO_2 (aq) according to Eq. (1); aqueous CO_2 reacts with H_2O and forms H_2CO_3 according to Eq. (2). The H_2CO_3 dissociation products ionise and form CO_3^{2-} and H_2O according to Eqs. (3 and 4). Ca^{2+} ions then need to be supplied to react with CO_3^{2-} (Eq. 5) to form $CaCO_3$ (Mwandira et al. 2023c):

$$CO_2(g) \leftrightarrow CO_2(aq) \tag{1}$$

$$CO_2(aq) + H_2O \leftrightarrow H_2CO_3 \tag{2}$$

$$H_2CO_3 \leftrightarrow H^+ + HCO_3^- \tag{3}$$

$$2HCO_3^- + 2OH^- \leftrightarrow 2CO_3^{2-} + 2H_2O \tag{4}$$

$$Ca^{2+} + CO_3^{2-} \leftrightarrow CaCO_3 \downarrow \tag{5}$$

Based on life cycle assessment studies, the carbonic anhydrase metabolic pathway was found to be the most sustainable pathway in comparison to other biocementation pathways, in terms of $CaCO_3$ production (Porter et al 2021). There are, however, very limited studies on CA biocementation for ground improvement with inconclusive results (see the literature review by Mwandira et al 2023b).

To address this knowledge gap, this research builds on the promising results of work presented at the CEMEPE10 conference by Mwandira et al. (2023d) studying the ability of CA-producing bacteria in precipitating calcite and biocementing soil, by adding CO_2 in the form of bicarbonate. This can be relevant to the method of capturing industrial CO_2 in the form of bicarbonate (Vaughan 2022). The particular novelties of this research are (a) the isolation of CA producing bacteria which are naturally occurring in the soil to be biocemented and the in-depth microbiological study and molecular characterisation of the isolates and (b) the proof of the optimised treatments presented in this study, towards fine-grained soil biocementation (other researchers only studied sand soil CA biocementation). By proving soil biocementation using the CA pathway, this research contributes to developing an eco-friendly biocementation technique with the advantage of stabilising the soil, which is used as a carbon sink for captured waste CO_2 during the stabilisation process. The research thus actively aligns with the extensive efforts for climate change mitigation and adaptation as it allows for simultaneously decarbonising the ground engineering industry and enhancing the resilience of civil infrastructure.

Materials and methods

Soil

The sample originated from 0.6 to 1.1-m depth above the groundwater table; it was extracted from a trial pit next to a railway embankment in Prickwillow, UK (the same geo-location as in Mwandira et al 2023a but a different depth). The soil from this layer was fine-grained but not plastic, unlike deeper soil layers of the same site (studied e.g. in Mwandira et al 2023a). Its particle size distribution (PSD) based on sieving and then hydrometer testing (BSI 2022a) is shown in Fig. 1. Material characterisation of the soil based on SEM–EDS analysis is shown in Fig. 2.

From duplicate samples, the soil was found to have a pH of 7.15 (suspended in distilled water and tested according to BSI, 2005), a natural gravimetric moisture content of 32.4% (tested according to BSI, 2022b), an organic content of 7% (tested according to ASTM 2014) and a natural $CaCO_3$ content of 4.77% (tested according to ASTM 2021). Based on these characteristics, our first assessment was that although the soil did not have a high organic content (unlike other foundation soil layers in the area, e.g. in Safdar et al 2021a,b & 2022) which can be potentially challenging for biocementation, the fine-grained size of the soil still poses potential challenges for biocementation treatment compared to sands (sands constitute the predominant soil type in the majority of other research and field applications of biocementation). The low hydraulic conductivity of fine-grained soils renders the flow and transport of the treatment solutions difficult, and for bioaugmentation, the precultured bacteria implemented into the soil must be able to pass through the narrow pore throats of the fine-grained soil, which would need to be bigger than the size of the bacteria.
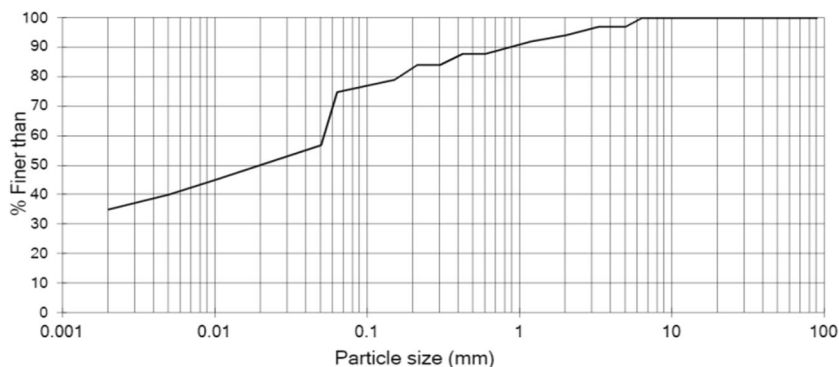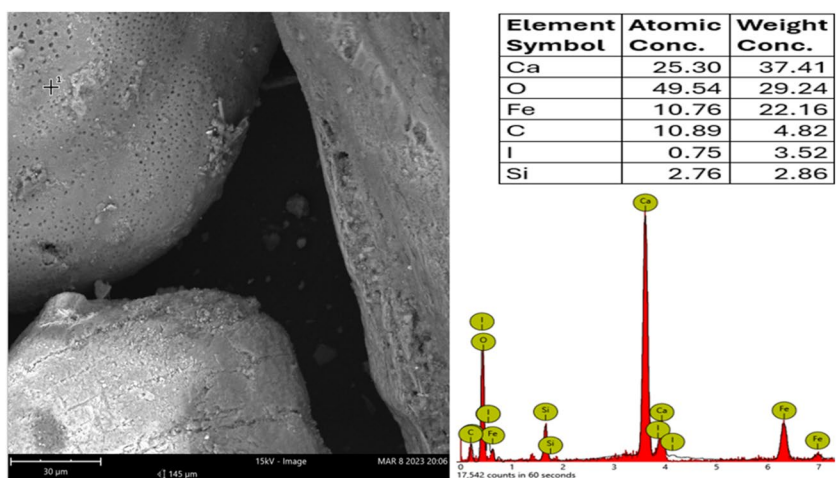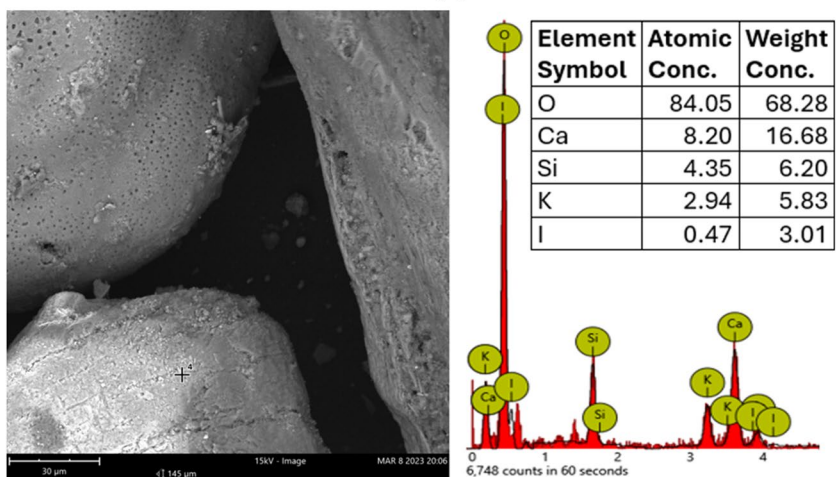
Fig. 1 PSD of soil

Fig. 2 **a**, **b** Material analysis of the untreated soil based on SEM and EDS indicatively shown on two different sites of the soil sample (see photos **a** and **b** respectively)

Element Symbol	Atomic Conc.	Weight Conc.
Ca	25.30	37.41
O	49.54	29.24
Fe	10.76	22.16
C	10.89	4.82
I	0.75	3.52
Si	2.76	2.86

(a)

Element Symbol	Atomic Conc.	Weight Conc.
O	84.05	68.28
Ca	8.20	16.68
Si	4.35	6.20
K	2.94	5.83
I	0.47	3.01

(b)

Microbiological study

Isolation and characterization of CA-producing microbes

The microbes found to produce CA were isolated from 1 g of soil placed in 10-ml deionized, sterile water and homogenized using a vortex mixer. The soil suspension was serially diluted to 10^{-4} using sterile deionised water, and 0.1 ml of the dilution was plated out on peptone agar medium containing 3 mM of *p*-nitrophenyl acetate (referred to as p-NPA), an indicator of CA-positive microbes. Colonies able to produce CA generated an intense yellow colour as p-NPA hydrolysed into para-nitrophenol (pNP). The plates were put in an incubator

at 30 °C for 72 h. After incubation, the soil yielded 40 CA-producing bacteria with different morphologies. An initial identification of microorganisms was performed using MALDI-TOF/TOF MS proteomic-based biotyping with a Bruker Daltonics MALDI Biotyper as described in Mwandira et al (2023a).

Bacterial growth, CA enzyme production and characterization

Of the 40 isolates showing CA activity, a preliminary screening based on the intensity of the yellow colour was carried out. The best three strains were selected for further study and quantification of their enzymatic activities. These three strains were preliminarily labelled as strain U-1, strain U-21 and strain U-26 until further identification through DNA sequencing, as described below. Pure single colonies of the three strains were aseptically inoculated in nutrient broth (50 ml) and incubated at 37 °C for 24 h. A 37 °C temperature was chosen based on the temperature identified for optimal CA enzyme activity elsewhere in the literature (Mwandira et al. 2023d). We determined CA colourimetrically (see Martin et al. 2009). Namely, the activity for p-nitrophenyl acetate hydrolysis was assessed using 1.35 ml of reaction mixture with 3 mM p-nitrophenyl acetate in phosphate buffer (0.13 M and pH 7.2) at room temperature. The reaction continued for 5 min, and the optical density (OD) change at 348 nm was measured using UV–Vis spectrophotometry. The quantity of p-nitrophenol generated per unit of time was used to characterise the CA enzyme activity as in Nathan and Ammini (2019):

$$CA\ activity\left(\frac{\text{U}}{\text{ml}}\right) = \frac{(\Delta A_{348}T - \Delta A_{348}B) \times 1000}{5 \times Volume} \quad (6)$$

where $\Delta A_{348}T$ is the final absorbance reading; $\Delta A_{348}B$ is the initial uncatalyzed reaction at a 348-nm wavelength. Volume is the volume of bacterial suspension added to the cell. 1 U (μmol/min) is the amount of the enzyme catalysing the conversion of 1 mM of substrate per min.

To determine the intracellular versus extracellular activity, the following method was used: 10 ml of bacteria culture was placed in a centrifuge tube (1) and centrifuged in 8000 rpm for 5 min. Following this, pellet cells were lodged at the bottom of the tube (tube 1) whilst the solution remaining in the tube (supernatant) was transferred to another centrifuge tube (tube 2). PBS buffer was then added to the pellet cells in tube (1), and it was mixed and shaken. Tube (1) was then sonicated at a 37 Hz frequency for 5 min; it was then again centrifuged at 8000 rpm for 5 min. The enzyme was then measured in both tube (1)

containing the cells and tube (2) containing the supernatant to determine the intracellular and extracellular enzyme, respectively, following the method used for finding the CA enzyme using a spectrophotometer as described earlier.

Optimisation of CA activity

To optimise CA activity, we performed an investigation of the effect pH, temperature, zinc cofactor and the molarity of the cementation solution (consisting of calcium acetate and sodium bicarbonate) on the growth of the bacteria and enzymatic activity. Bacterial growth was determined using UV–Vis spectrophotometry that recorded OD readings at 600 nm for 96 h. Following sterile inoculation, we cultured the medium at a constant temperature oscillation incubator (120 rpm) at 5 ℃, 15 ℃, 25 ℃, 30 ℃ and 37 ℃ respectively for 24 h before measuring the OD_{600} value and CA in the medium solution. Similarly, the effect of the pH was measured for a range of pH = 6–11 by adjusting the pH using NaOH solution and measuring the OD_{600} and CA in the solution as described previously. Finally, the effect of zinc acting as a metallocofactor for CA was evaluated by adding Zn to the assay reaction mix at concentrations of 0, 1, 5, 10 and 20 mM respectively. The enzyme activity was then determined according to Eq. (6) for different Zn concentrations. The tests were performed in triplicate.

An additional investigation examined the effect of the source of calcium (i.e. calcium salt supplied) on bacterial growth and enzymatic activity. This investigation was carried out indicatively for one of the selected strains, namely U-1.

DNA sequencing and analysis

The three selected strains (labelled respectively as strain U-1, strain U-21 and strain U-26) were prepared for sequencing. For each of the three strains, a 1-ml overnight culture was pelleted and resuspended in 600-μl 50 mM EDTA containing 120-mg lysozyme (Sigma-Aldrich, St. Louis, USA). DNA was then extracted using a Promega Wizard Genomic DNA purification kit using the manufacturer's protocol for Gram-positive bacteria. We assessed the extracted DNA quality and quantity using a NanoDrop spectrophotometer (supplied by ThermoFisher Scientific) and a Genomic DNA ScreenTape essay on a TapeStation 4200 System (Agilent, Santa Clara, USA). The DNA samples were shipped in ice-packs to Novogene (Cambridge, UK) for library preparation and sequencing. In brief, before Illumina adapters were ligated, the DNA was fragmented, end repaired and A-tailed. The ligated fragments were size-selected, PCR amplified and purified to obtain the final libraries. The libraries

(insert + adapters length: 320–520 bp) were sequenced on an Illumina NovaSeq 6000 (paired-end; 2*150 bp).

We processed raw reads using Trimmomatic v0.39 (Bolger et al [2014](#)), removing remaining adapters and any 5′ and 3′ bases with a quality value below 20. IDBA was used to assemble the remaining sequence reads (Peng et al [2012](#)) with '*mink*' set to 80 and '*maxk*' set to 124, but otherwise default settings. The genomes were annotated using pgap (Tatusova et al [2016](#); quality and contamination scores of the three genome assemblies were determined using Quast (Gurevich et al [2013](#)) and CheckM (Parks et al [2015](#))), respectively. The assembled genomes were combined with chromosome-level assembled, full-length *Bacillaceae* genomes (downloaded from the NCBI Datasets database on 02 Nov. 2023) for phylogenetic reconstruction using the GToTree (Lee [2019](#)) pipeline, allowing for steps to be run in parallel (Tange [2018](#)). For this, 74 single-copy orthologues were targeted using HMMER3 (Eddy [2011](#)) and the provided 'Bacteria' HMM file. Before concatenating, the gene sequences were translated using Prodigal v2.6.3, aligned using Muscle 5.1 (Edgar [2004](#)), trimmed using TrimAl v1.4 (Capella-Gutiérrez et al [2009](#)). Then, phylogenetic analyses were performed using FastTree Version 2.1.11 (see Price et al. [2010](#)) (a JTT model of protein evolution, CAT rate approximation with 20 rate categories, and Shimodaira-Hasegawa test with 1000 bootstrap replicates to calculate support values). TaxonKit (Shen and Xiong [2019](#)) was used to retrieve and add NCBI taxonomy info to the taxon labels. The tree was visualised and formatted using FigTree v1.4.4 (Rambaut [2018](#)). Putative carbonic anhydrase genes were pinpointed by searching the pgap annotations.

CaCO$_3$ production in aqueous solution

Bioprecipitation due to the selected isolates was examined using equimolar solutions of sodium bicarbonate and calcium acetate (0.1, 0.25, 0.5, 0.75 and 1.0 M respectively). Note that for the main investigations, we used sodium bicarbonate to obtain the required CO$_2$ instead of CO$_2$ directly injected to the soil. The bacterial isolates were precultured for 24 h in 10-ml liquid nutrient medium. The nutrient medium composition is shown in Table [1](#). We incubated aerobically inoculant solutions at 37 °C for 48 h with 120 rpm shaking; we then inoculated 1 ml of preculture into broth

Table 1 Nutrient medium composition

Ingredient	Quantity (g/l)
Peptone	5.0
Sodium chloride	5.0
Beef extract	1.5
Yeast extract	1.5

(100 ml) and grew the inoculum at 37 °C for 96 h with continuous aeration at 120 rpm. The overnight microbial culture was diluted to 0.5 MacFarland standard to reach a cell concentration of 9×10^8 cells/l at OD$_{600}$; this concentration was subsequently used in the bioaugmentation treatments using cementation solutions with the molarities mentioned above. The mixes were incubated at 30 °C for 6 h and shaken at 160 rpm; subsequently, to collect the precipitate, they were centrifuged at 15,000 rpm for 5 min. An additional qualitative investigation to attest the possibility of obtaining bioprecipitation due to atmospheric CO$_2$ capturing (without the use of bicarbonate) in 0.1 M calcium acetate solution was also performed in triplicate. Namely, the substrates were bioaugmented using the same cell concentration of 9×10^8 cells/l (one strain at a time) and following the same inoculation procedure as described earlier, however without attempting to control the ingress of other microorganisms in order to mimic the conditions of the soil on site. Calcium ion concentration in the medium was measured using a Horiba LAQUATwin calcium ion meter.

Material analysis

We used scanning electron microscopy (SEM) to inspect the microstructure of the biominerals formed. It was carried out using a ThermoScientific Pharos FEG-SEM with high vacuum mode and 15 kV acceleration voltage. We performed energy-dispersive x-ray spectroscopy (EDX) analysis using a Silicon drift detector (SDD) and 30-s integration time. Furthermore, the bioprecipitates were analysed by a Cary 630 FTIR spectrometer (Agilent Technologies) with range 600–4000 cm^{-1} and resolution of 4 cm^{-1}. Raman spectroscopy was carried out to identify the bioprecipitates using a Horiba LabRAM ARAMIS confocal Raman microscope (50X objective, 633-nm laser − 1% power, 100-μm pinhole, 600 l/mm grating).

Testing for soil biocementation

Specimens of 100-mm height and 50-mm diameter were compacted at a dry density of 1.34 g/cm^3 (which was the dry density of the soil in the field) and at the natural gravimetric soil water content. A 2-stage injection was used to implement the treatments: first, the bacteria (cell concentration of 9×10^8 cells/l) were injected (stage 1), followed by the cementation solution (in this instance, 0.1 M Ca(CH$_3$COO)$_2$ and NaHCO$_3$ solutions) (stage 2). Solutions were injected by syringe into the top of the soil specimens. A two-stage injection was deemed preferable to allow bacteria to attach to the particles before cementing solution is sent through (thus creating nucleation sites for subsequent calcite precipitation) but also to prevent calcite formation in the syringe before injection in the soils as the CA-induced chemical

reaction was observed to be very fast. Specimen curing lasted 14 days. As the untreated (control) specimens were not sufficiently cohesive to test in unconfined compressive strength testing apparatus and were crumbling as soon as compression was applied, the approximate unconfined compressive strength of all specimens (treated and untreated) was tested using a pocket penetrometer. After pocket penetrometer testing, samples across the specimen were collected and their oven-dried masses determined. They were then subjected to acid wash using a 2 M HCl solution, oven-dried and their mass measured again. The difference in these two oven-dried masses was identified as the $CaCO_3$ mass produced by biocementation. Filter paper was used while rinsing repeatedly the dissolved $CaCO_3$ and HCl solution to flush the dissolved salts out the soil without losing the soil particles.

Results and discussion

Microbiological study

Isolated strain identification—DNA sequencing results

The 40 CA-producing bacteria were subjected to preliminary identification at the end of the incubation period, based on MALDI-TOF testing. All strains that returned MALDI-TOF matches of secure or probable genus identification were identified as of the *Bacillus* genus. The three selected strains were then identified by DNA sequencing. In total, 3,991,848 (for U-1), 3,417,220 (for U-21) and 4,663,946 (for U-26) read pairs were generated, and of these read pairs, 3,987,295 (99.89%), 3,360,137 (98.33%) and 4,606,773 (98.77%) passed the quality control step. The data was assembled and assembly quality assessed. The U-1 assembly consists of 86 contigs with total length of 4,171,408 bp, a N50 of 92,570, a GC% of 46%. Of the reads, 99.79% could be mapped back to the contigs, and the average coverage was 194. The U-21 assembly consists of 124 contigs with a total length of 3,877,410 bp, a N50 of 67,646, a GC% of 41%. Of the reads, 99.76% could be mapped back to the contigs, and the average coverage was 176. The U-26 assembly consists of 286 contigs with a total length of 6,217,871 bp, a N50 of 70,265, a GC% of 35%. Of the reads, 99.86% could be mapped back to the contigs, and the average coverage was 150. The genomes were annotated and completeness estimated using CheckM (U-1: 98.86%; U-21: 95.61%; U-26: 99.31%), which also revealed low contamination (U-1: 1.20%; U-21: 3.53%; U-26: 0.54%). Strain heterogeneity was estimated to be 5.26% for U-1, 3.70% for U-21 and 75% for U-26. The CheckM genome completeness estimates were corroborated by HMMER searches, which also indicated that the genomes are largely complete: Of the 74 genes included in the phylogenetic analysis, 73 were recovered for U-1 (with 0% redundancy) and U-21 (with 1.35% redundancy). All 74 genes were recovered for U-26 (with 5.41% redundancy). These values are within the range seen for the 116 genomes that were downloaded from the NCBI Datasets database (for genome summary, see supplementary material in Online Resource 1a). The final data matrix had a length of 12,444 amino acids and was used for phylogenetic tree reconstruction. The robust placement of the strains in the tree (Fig. 3) suggests that U-1 is *Bacillus licheniformis*, U-21 is *Bacillus pumilus* and U-26 is part of the *Bacillus cereus* group and most likely is *Bacillus toyonensis*. U-1 and U-21 have five and three CA, respectively. This is similar to the reference genomes in the NCBI databases (*Bacillus licheniformis*: GCF_002074095.1, *Bacillus pumilus*: GCF_003020795.1). U-26 has five CA. The *B. toyonensis* reference genome (GCF_016605985.1) in NCBI databases has only four CA annotated, but checking using blast the five CA are all found in other publicly available *B. toyonensis* strains. The protein sequences are shown in Table S1 of supplementary material (Online Resource 2).

Bacterial growth and CA enzymatic activity

The results of microbial growth, CA enzyme activity and Gram stain of *B. licheniformis* (U-1), *B. pumilus* (U-21) and *B. toyonensis* (U-26) are summarised in Fig. 4 a–d. The microbial growth curves (Fig. 4a) show the typical lag, exponential, stationary and death phases. Maximum growth was observed at 24 h for *B. licheniformis* and at 48 h for *B. pumilus* and *B. toyonensis*.

Figure 4 b shows that *B. licheniformis*, *B. toyonensis* and *B. pumilus* had high specific carbonic anhydrase enzymatic activity (respectively 1.39, 1.42 and 1.50 U/ml) and can be used for biocementation. The CA activity of the isolated strains is higher than that reported for *B. schlegelii* isolated from garden soil (0.0453 U/ml) (Nathan and Ammini 2019) and *B. altitudinis* isolated from mangrove sediments (0.695 U/ml) (Muley et al 2014). However, the three isolates showed a lower CA activity compared to *Bacillus* sp. AP6 (5.61 U/ml) and *Bacillus mucilaginosus* used respectively for biocementation and CO_2 capture (Achal and Pan 2011). In general, *Bacilli* species were found to be tolerant to high CO_2 concentrations in previous investigations (see e.g. Hu et al 2020). The three isolates are thus good candidates for both carbon sequestration and biocementation applications.

The results of the intracellular and extracellular enzyme activities (Fig. 4d), which were determined to elucidate the mechanism by which the isolates secrete CA, show that consistently with Klier et al. (2014), the isolates can secrete both intracellular and extracellular CA and can thus be also used to produce crude CA for biocementation applications.

Fig. 3 Results of maximum likelihood-based phylogenetic analysis of 119 Bacillaceae including the three selected isolates (U-1, U-21, U-26). The tree is based on 74 translated and concatenated protein coding gene sequences and was rooted on *Lysinibacillus*. No support values are shown; Phylogenetic tree with support values is provided as supplementary material (Online Resource 1b)
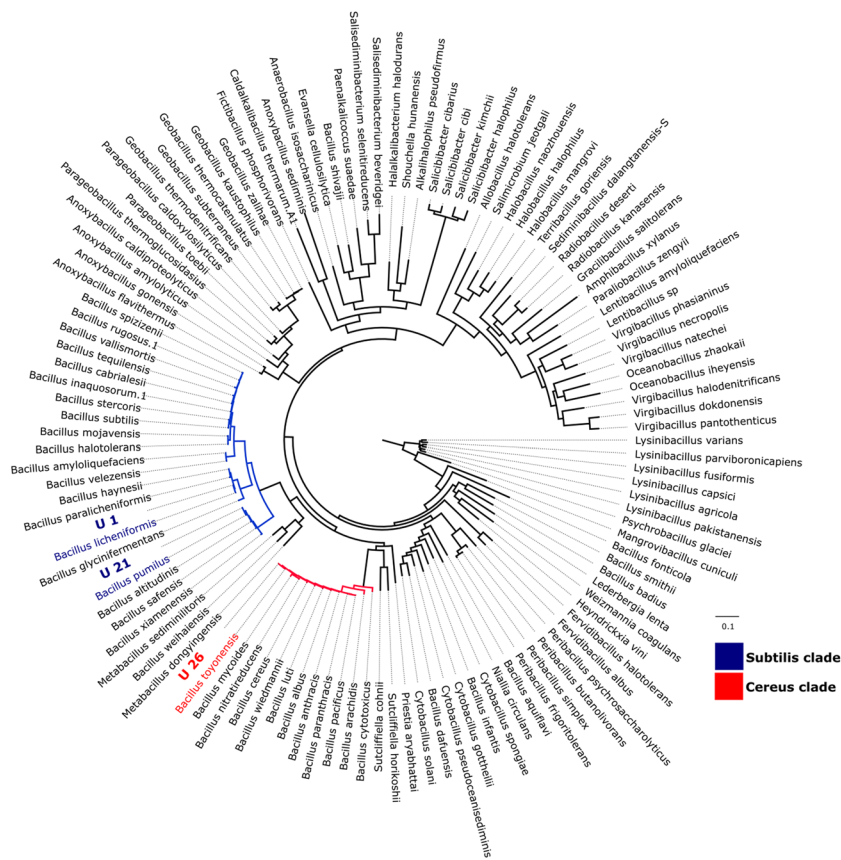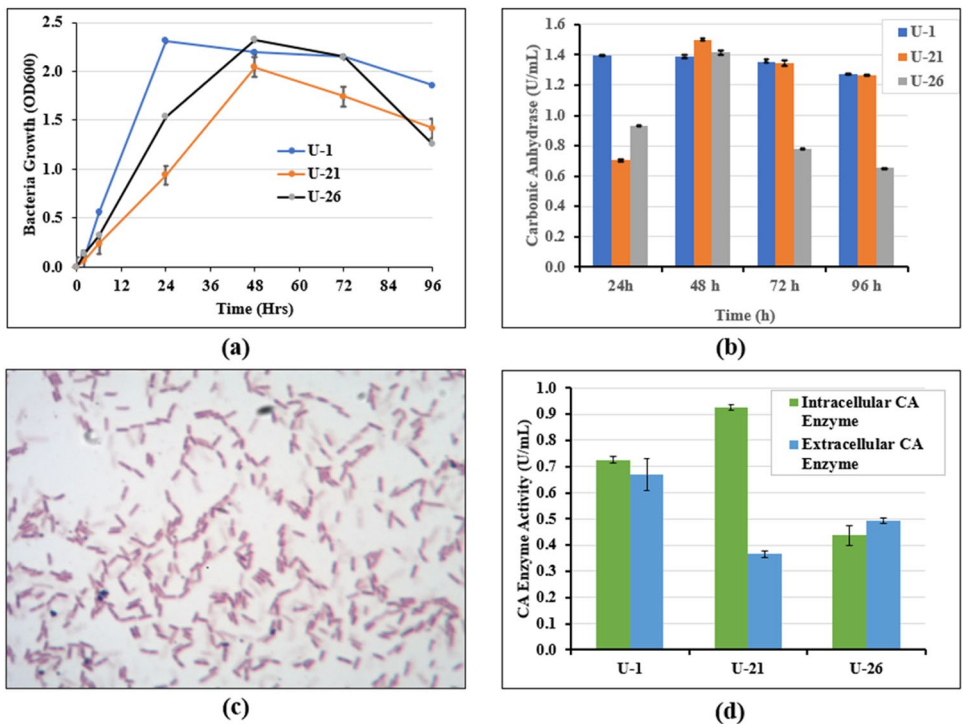

Fig. 4 Bacterial growth and CA activity: **a** microbial growth curves; **b** variation of CA activity in time; **c** indicative gram-stained photo of *B. pumilus* isolate; **d** intracellular and extracellular CA activity

Optimization for CA production

Three factors were optimised to determine the most optimal parameters for the growth of the selected strains, namely, pH, temperature, and Zn cofactor addition (Fig. 5a–d). Figure 5 a shows that all three isolates had lower CA activity at temperatures higher than 50 °C or lower than 25 °C; optimal microbial growth was observed at 37 °C. However, temperatures below 20 °C, which would be most common in the soils in situ, appeared to have little effect on the comparative activity of the different bacteria. Figure 5 b shows that all three bacteria could grow at pH 6, 7 and 8; however, only *B. licheniformis* could grow at pH 9–10, but no growth was observed for *B. licheniformis* at pH values > 11. The optimal pH for *B. licheniformis*, *B. pumilus* and *B. toyonensis* was determined as pH 9 (where CA activity increased to 1.79 U/ml), pH 6 and pH 7 respectively.

Figure 5 c shows the effect of supplementing Zn cofactor for improving CA production. As shown in the figure, there was an approximate 40% increase in CA production in *B. pumilus* and *B. toyonensis* when cofactor was added at increasing concentrations, optimally at a dosage of 10 mM Zn^{2+}. A previous study (Jaya et al. 2019a, b) similarly reported that 10 mM Zn^{2+} improved the growth of *B. altitudinis* M8 strain isolated from the mangrove soil microcosm. The increased microbial growth and CA production upon Zn addition as a cofactor has been attributed to the fact that Zn ions are able to stabilise the structure of CA enzyme by resisting electrostatic repulsion (see e.g. Tu et al. 2012). Interestingly, however, no increase was shown in *B. licheniformis*; in fact, the results imply that Zn addition inhibited microbial growth. All subsequent investigations in this study used the optimized conditions for each strain in terms of pH, temperature and Zn cofactors based on this investigation.

Furthermore, Fig. 6 shows that calcium acetate was more favourable than calcium chloride in terms of bacterial growth and enzymatic activity for the solution concentrations tested, possibly as it acts as an additional source of carbon for the bacteria.
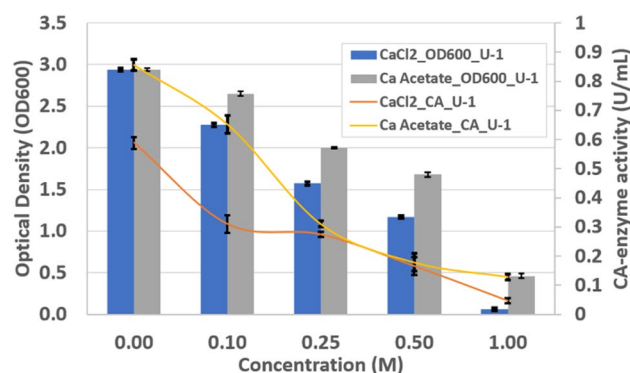

Fig. 6 Impact of different calcium sources on the growth and CA activity of *B. licheniformis* (U-1)

CaCO₃ bioprecipitation results

CaCO₃ bioprecipitation was studied to assess if the three isolated strains can potentially biocement soil. Figure 7 shows the quantity of deposited Ca^{2+} using different molarity cementation solutions for *Bacillus licheniformis*, *Bacillus pumilus* and *Bacillus toyonensis*, respectively. Deposited bioprecipitated Ca^{2+} increased as solution concentration increased in comparison to purely chemical reaction precipitate, in particular for *Bacillus licheniformis* although for the other two strains, the difference with comparison to the chemical reaction precipitates became smaller as solution concentrations increased. The higher deposited Ca^{2+} amount compared to the purely chemical reaction could be due to the fact that microbial cells become nucleation sites for the crystallisation of CaCO₃ (Aloisi et al 2009). However, the marginal increase in deposited Ca^{2+} compared to the purely chemical reaction at higher molarities at least for *Bacillus pumilus* (U-21) and *Bacillus toyonensis* (U-26) could be due to enzymatic activity inhibition in solutions of high calcium ion concentrations, as reported in the literature (Whiffin 2004). Zheng and Qian (2020) explained that high Ca^{2+} concentrations increase osmotic pressure around
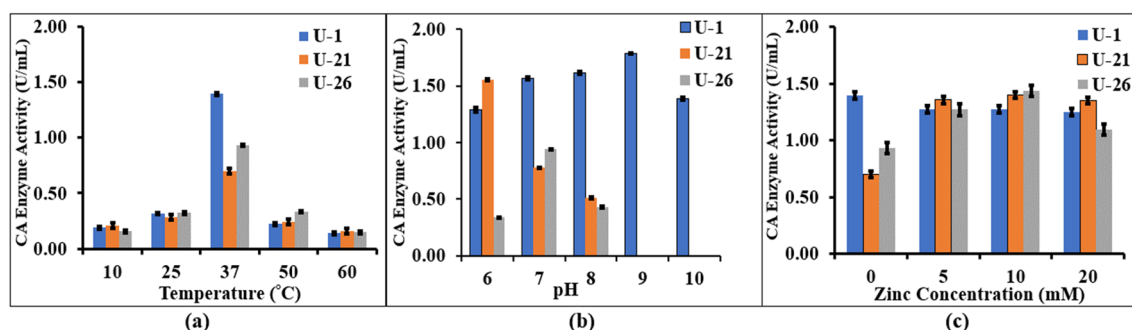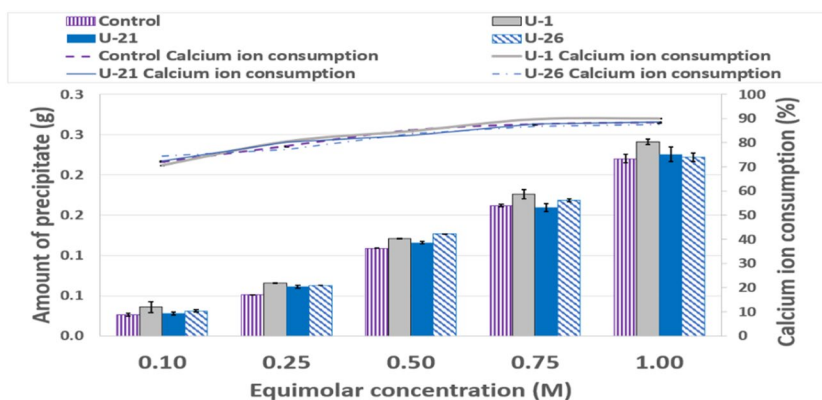

Fig. 5 Impact of different factors on CA enzyme activity of the three isolates: **a** effect of temperature, **b** effect of pH, **c** effect of Zn as a cofactor on the three isolates. Values shown are mean ± SD (*n* = 3)

Fig. 7 Deposited Ca.$^{2+}$ at different cementation solution concentrations for *Bacillus licheniformis* (U-1), *Bacillus pumilus* (U-21), and *Bacillus toyonensis* (U-26)

the bacteria cell membrane, triggering flow from low to high Ca^{2+} concentration areas through the cell membrane. This causes cell dehydration and plasma wall separation; microbes may thus stop growing and die. Additional investigations of bioprecipitation by ureolytic bacteria isolated from the soil in 1 M cementing solutions showed that the CA route compared favourably against the ureolytic route in terms of precipitate amount (Online Resource 3).

SEM was used to confirm the CaCO$_3$ bioprecipitation at different cementing solution molarities; the results are shown in Fig. 8, which clearly demonstrate that cementation solution concentration affects the crystal morphology and size. The purely chemical reaction of sodium bicarbonate and calcium acetate (labelled as "control" analysis in Fig. 8a–c) produced mainly rhombohedral calcite crystals at low molarities; at higher molarities, some more spherical crystals and amorphous phases are also noted. Bacteria produced different bioprecipitates. For *Bacillus licheniformis* (U-1) (Fig. 8 d–f) at low molarities, rhombohedral crystals were also observed, but more spherical crystals were observed at higher molarities probably denoting the presence of vaterite, a more unstable CaCO$_3$ phase. For *Bacillus pumilus* (U-21) (Fig. 8 g–i) and *Bacillus toyonensis* (U-26) (Fig. 8 j–l), the formation of calcite at low molarities is less well pronounced; at intermediate molarities, spherical precipitates are again observed whereas at 1.0 M concentration, crystal morphology was more irregular with various forms of crystals, including some needle-like crystals especially for *Bacillus toyonensis* (U-26) which are more consistent with the morphology of aragonite crystals. EDS analysis, with indicative results shown in Fig. 9, confirmed the CaCO$_3$ formation (see elemental composition at indicative spots on the respective SEM samples).

Raman analysis results in Fig. 10a also showed spectra dominated by carbonates/calcium carbonate (calcite)-like signals in particular the highest shift intensity at 1088 cm^{-1}, which indicates that carbonate minerals are present. It can be noted that the spectra of typical bioprecipitates as well as the control (purely chemical precipitate formation) match typical calcite spectra, e.g. the primary peaks at 1088 cm^{-1} but also those at 280 cm^{-1} and 153 cm^{-1} and 715 cm^{-1}, indicating that the bioprecipitates are calcite (see also similar results in other microbially induced carbonate precipitation studies, e.g. Bai et al 2017). The Raman spectra results demonstrate that calcite was formed using CA-producing bacteria from the selected isolate from the soil. FTIR analysis (Fig. 10(b)) further confirms carbonate formation, and in particular calcite; in particular, C–O stretching vibrations around 1400 cm^{-1} indicate CO$_3^{-2}$ presence in both control and bioprecipitates; single peaks at around 1400, 870, 713 and 745 cm^{-1} are all observed in the standard calcite spectra indicating that CaCO$_3$ in the form of calcite has apparently formed.

The results of the bioprecipitation due to atmospheric CO$_2$ capture (i.e. without the use of bicarbonate) are shown in Fig. 11. They report on the monitoring of bioprecipitation via electrical conductivity, pH and calcium concentration measurements in the medium in time. It is worth noting that in order to mimic site conditions, the bioaugmented substrates were exposed to the atmosphere, and sterility was not maintained. From Fig. 11, it can be seen that all bioaugmented samples manifest a change in their electric conductivity and calcium content indicating the formation of precipitation products; the sample which shows the most pronounced change in both electrical conductivity and calcium content for the first 6 days of exposure is that bioaugmented with *B. licheniformis*; the sample bioaugmented with *B. toyonensis* also mirrors closely the patterns of EC and calcium concentration change of the control mix (chemical reaction without bioaugmentation) although the change in EC is more pronounced compared to that of the control mix. On the other hand, the consumption of calcium ions does not happen at the same time as the EC change, and it also appears to be completed earlier than in the control mix.
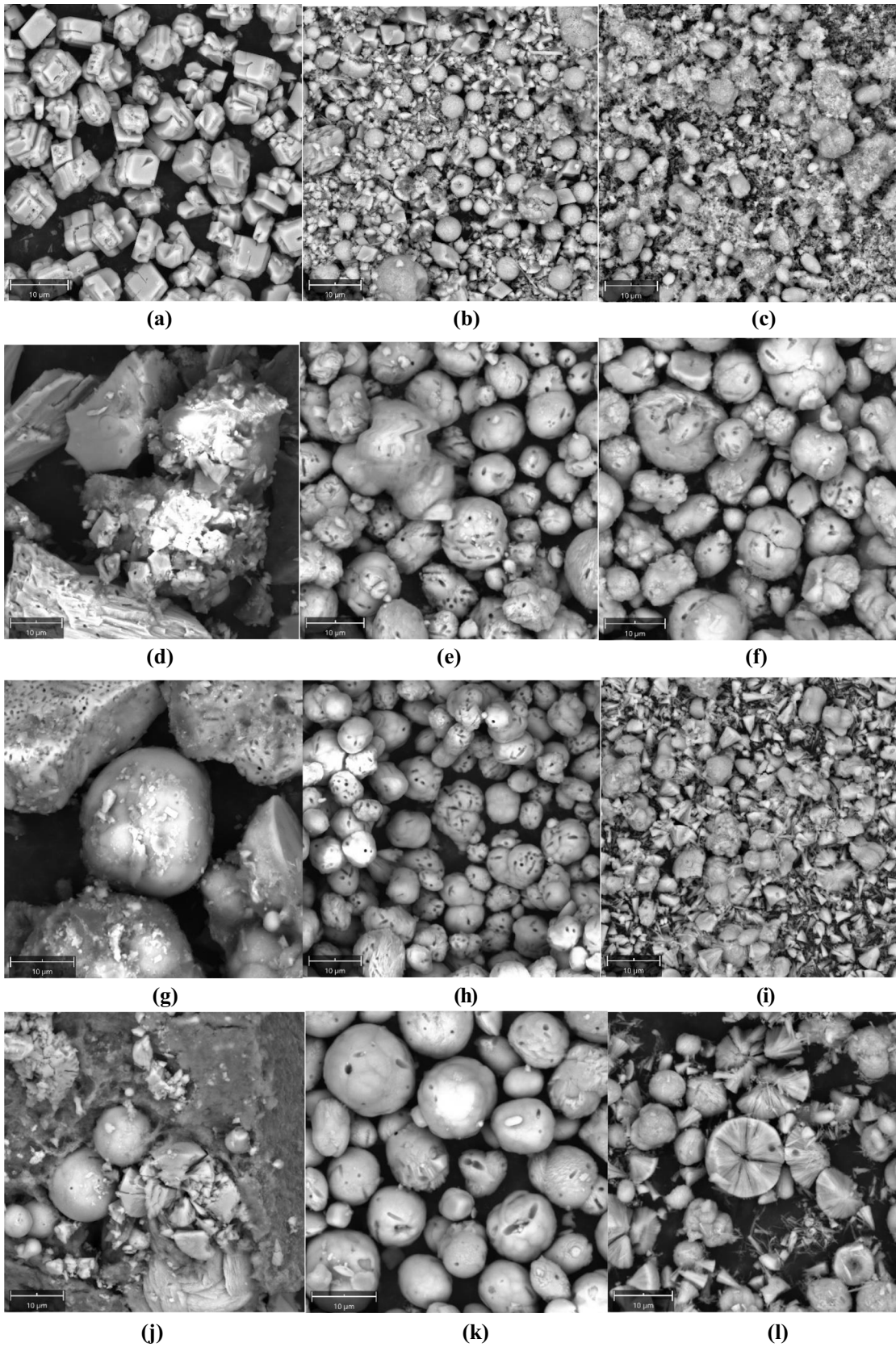
(a) **(b)** **(c)**

(d) **(e)** **(f)**

(g) **(h)** **(i)**

(j) **(k)** **(l)**

◀ **Fig. 8** SEM results at different cementation solution molarities: **a–c** control, 0.1 M, 0.5 M, 1 M respectively; **d–f** *Bacillus licheniformis* (U-1), 0.1 M, 0.5 M, 1 M respectively; **g–i** *Bacillus pumilus* (U-21, 0.1 M, 0.5 M, 1 M respectively; **j–l** *Bacillus toyonensis* (U-26), 0.1 M, 0.5 M, 1 M respectively

Soil biocementation

To prove soil biocementation, pocket penetrometer readings were taken at various parts of the injected specimens (Fig. 12a); the calcite content of the same specimens was then measured (Fig. 12b). From the figure, it can be seen that unconfined compressive strengths of 1 MPa and 0.5 MPa were obtained respectively at the top and middle of specimens treated with *B. licheniformis*. An increase of calcite content of 2.78% and 0.57% was noted respectively at the top and middle of specimens; this is consistent with crystals forming on the treated specimen surface (Fig. 12b), unlike the untreated soil specimen. However, the bottom of the treated specimens showed no evidence of biocementation, as no increase in calcite content was observed and pocket penetrometer testing was unfeasible (same as for the untreated soil specimens) because the bottom of the specimens lacked in cohesion and crumbled upon testing. Immersion of samples in water for 1 day proved that the strengths recorded for the top and middle of the specimens were due to

Fig. 9 Indicative SEM–EDS results confirming CaCO$_3$ precipitation: **a**, **b** control; **c**, **d** *Bacillus licheniformis* (U-1); **e**, **f** *Bacillus toyonensis* (U-26)

(a)

(b)

(c)

(d)

(e)

(f)
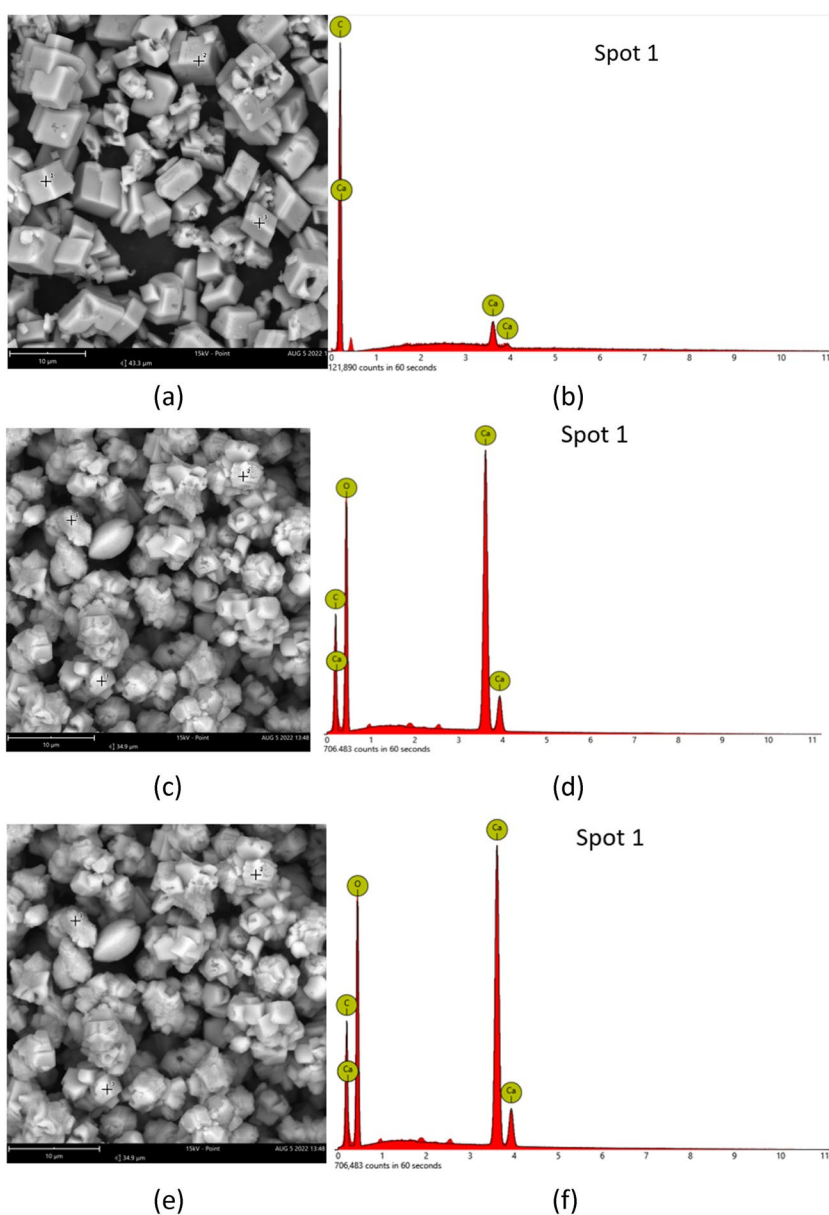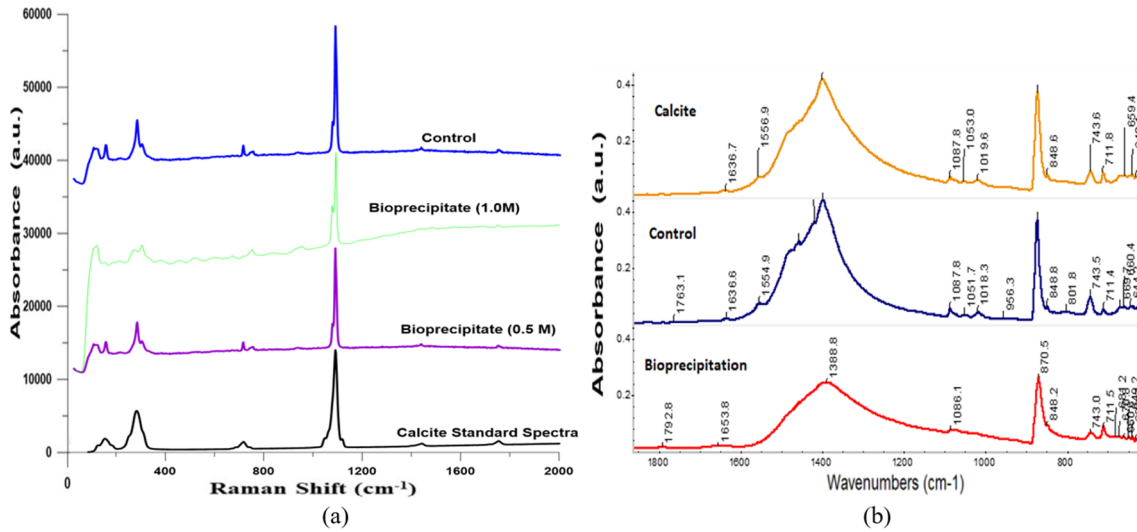
Fig. 10 a Raman spectra of control, bioprecipitate and calcite standard spectra. **b** FTIR spectra of control, bioprecipitate and calcite standards spectra (a.u. stands for 'arbitrary units')

Fig. 11 Bioprecipitation indicators due to atmospheric CO_2 capture for the control mix (mostly chemical reaction—no bioaugmentation) and for bioaugmented samples, respectively, with *Bacillus licheniformis* (U-1), *Bacillus pumilus* (U-21) and *Bacillus toyonensis* (U-26): **a** electrical conductivity; **b** calcium concentration in the medium; **c** pH of the medium

(a)

(b)

(c)

(d)
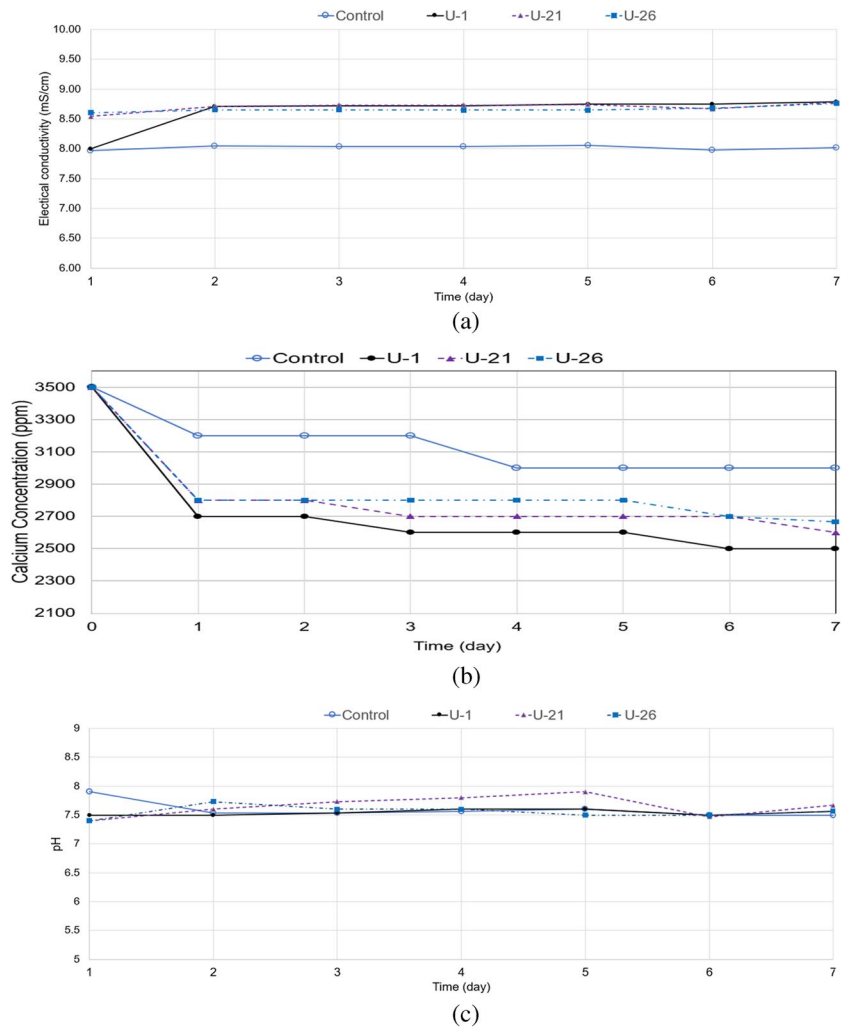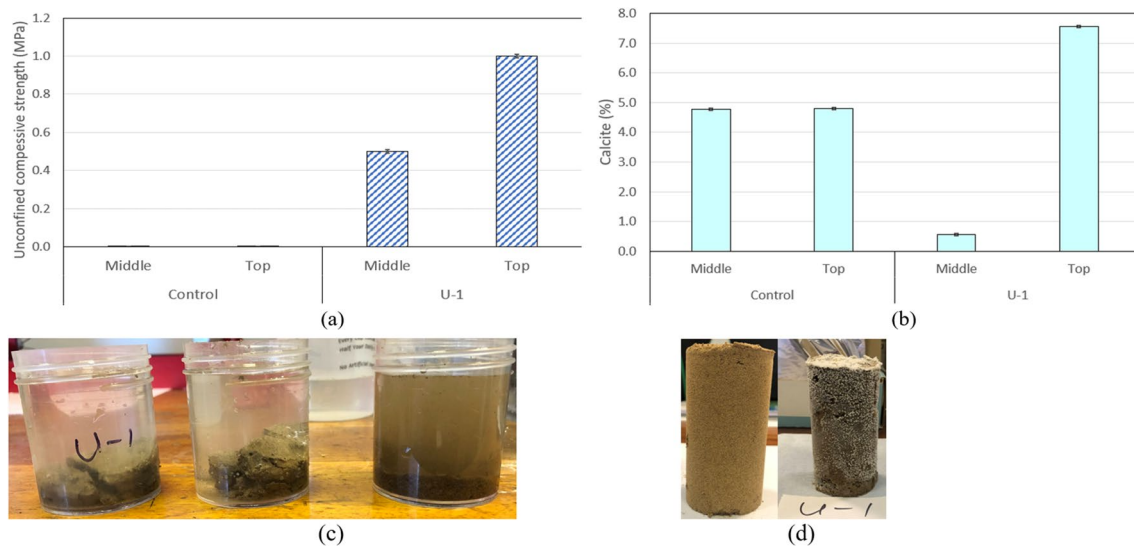
Fig. 12 Biocementation study specimens: **a** pocket penetrometer results (UCS); **b** calcite content; **c** immersion test results of soil treated with *B. licheniformis*: samples from top (left), middle (mid-dle) and bottom (right) of the soil specimen, respectively; **d** appearance of untreated (left) and treated (right) soil specimens

cementation rather than suction effects, as the soil samples remained intact after immersion in water; conversely, the samples coming from the bottom of the specimens disintegrated in water, consistently with the lack of biocementation (see Fig. 12a). The non-uniformity of biocement distribution in soils is a known problem when injection is used for the implementation of the treatments; in this case, it was also exacerbated because of the fineness (thus, low hydraulic conductivity) of the soil. For this reason, we are developing instead electrokinetic implementation techniques (see Mwandira et al 2023a), which were shown to result in much improved treatment uniformity for fine-grained soils (Safdar et al 2021b). In the present work, however, the aim was the proof of soil biocementation using the autochthonous CA-producing strains, rather than the development of appropriate implementation techniques, which are the focus of future work. Based on the obtained results, biocementation was proven for the parts of the specimens that treatments have reached.

Conclusion

This research work identified and studied carbonic anhydrase–producing bacteria isolated from a railway embankment foundation soil in East Anglia, towards future field biocementation application. The main focus of this paper was the study of the growth of the isolated autochthonous bacteria, the optimisation of carbonic anhydrase production and the study of bioprecipitates upon cementing solution implementation. Indicative results proving native

soil biocementation using one of these strains were also presented.

The main findings of the paper were that:

- Most strains with CA activity isolated from the native soil were of the *Bacillus* genus; three of the most promising strains in terms of growth and carbonic anhydrase activity were identified as *Bacillus licheniformis*, *Bacillus pumilus* and *Bacillus toyonensis*.
- The study showed that the three specific *Bacillus* bacterial strains were able to produce CA for biocementation and capture CO_2. Of these strains, *Bacillus licheniformis* had the added advantage of a more rapid growth (12 h) at a wider pH range, namely pH = 6–10, and did not require any Zn cofactor to enhance its activity.
- All three strains showed good intracellular as well as extracellular activity (an advantage if crude enzyme from bacteria was to be utilised) and had optimal CA activity at 37 °C.
- The results indicated that calcium acetate enhanced the growth of *Bacillus licheniformis* and its CA activity compared to calcium chloride for the range of molarities studied.
- Different bacterial strains and solution concentrations led to different bioprecipitate morphologies, but the presence of calcite was confirmed by material analysis.
- The bioaugmentation treatment with CA-producing bacteria considerably increased the UCS of the biocemented parts of the soil reaching up to 1 MPa of UCS and produced additional calcium carbonate of up to an extra

2.78% compared to that of the untreated soil. Immersion testing results concurred with soil biocementation.

- As CA homologues were present in the genome, these may be valuable for further functional analyses and studies to further understand the biocementation process with concurrent CO_2 sequestration.

Overall, the results show promise that the use of CA-producing bacteria can produce biocements while capturing CO_2 and that upon further development of soil treatment protocols and treatment implementation techniques, these biocements can be suitable to improve the engineering soil properties, including those of fine-grained soils. Achieving this would thus help decarbonise both the construction and maintenance of earthwork infrastructure, while making it more resilient to the effects of a changing climate.

Supplementary Information The online version contains supplementary material available at https://doi.org/10.1007/s11356-024-34077-0.

Declarations

Ethical approval Not applicable

Consent to participate Not applicable

Consent for publication Not applicable

Competing interests Professor Diane Purchase is a member of the Editorial board of the *Environ. Sci. Pollut. Res.* journal. There are no other non-financial or financial interests relevant to this article to disclose.

References

Achal V, Pan X (2011) Characterisation of urease and carbonic anhydrase producing bacteria and their role in calcite precipitation. Curr Microbiol 62(3):894–902. https://doi.org/10.1007/s00284-010-9801-4

Aloisi G, Gloter A, Krüger M, Wallmann K, Guyot F, Zuddas P (2009) Nucleation of calcium carbonate on bacterial nanoglobules. Geology 34(12):1017–1020. https://doi.org/10.1130/G22986A.1

Amarakoon GGNN, Koreeda T, Kawasaki S (2014) Improvement in the unconfined compressive strength of sand test pieces cemented with calcium phosphate compound by addition of calcium carbonate powders. Mater Trans 55(9):1391–1399

Astaraki F, Esmaeili M (2022) Slope stabilisation of railway embankments over loose subgrades using deep-mixed columns. Proc Inst Civ Eng Ground Improv 175:247–260. https://doi.org/10.1680/jgrim.20.00049

ASTM (2014) D2974 – 14: Standard Test Methods for moisture, ash, and organic matter of peat and other organic soils. ASTM International, West Conshohocken, PA, USA

ASTM (2021) ASTM D4373–21: Standard Test Method for rapid determination of carbonate content of soils. ASTM International, West Conshohocken, PA, USA

Bai Y, Guo X, Li Y, Huang T (2017) Experimental and visual research on the microbial induced carbonate precipitation by Pseudomonas aeruginosa. AMB Express 7:57. https://doi.org/10.1186/s13568-017-0358-5

Banaś A, Andrzej K, Lech B, Agnieszka P-O (2020) Innovative method of strengthening soil behind the abutment by using geopolymer injections. Builder 278:24–28

Bolger AM, Lohse M, Usadel B (2014) Trimmomatic: a flexible trimmer for Illumina sequence data. Bioinforma Oxf Engl 30:2114–2120

British Standards Institute (BSI) (2005) BS ISO 10390:2005 soil quality. Determination of pH, BSI, London, UK

British Standards Institute (BSI) (2022a) BS 1377–2:2022: methods of test for soils for civil engineering purposes - classification tests and determination of geotechnical properties, London, UK

British Standards Institute (BSI) (2022b) BS EN ISO 17892–1:2014+A1:2022 Geotechnical investigation and testing. Laboratory testing of soil Part 1: Determination of water content, BSI, London, UK

Capella-Gutiérrez S, Silla-Martínez JM, Gabaldón T (2009) trimAl: a tool for automated alignment trimming in large-scale phylogenetic analyses. Bioinformatics 25:1972–1973

Chittoori, B.C.S., Burbank, M., Islam, M.T., (2018) Evaluating the effectiveness of soil-native bacteria in precipitating calcite to stabilize expansive soils. American Society of Civil Engineers (ASCE), pp. 59–68. https://doi.org/10.1061/9780784481592.007

Coudert E, Paris M, Deneele D, Russo G, Tarantino A (2019) Use of alkali activated high-calcium fly ash binder for kaolin clay soil

stabilisation: physicochemical evolution. Constr Build Mater 201:539–552

Eddy SR (2011) Accelerated profile HMM searches. PLoS Comput Biol 7:e1002195

Edgar RC (2004) MUSCLE: multiple sequence alignment with high accuracy and high throughput. Nucleic Acids Res 32:1792–1797

Gomez MG et al (2017) Stimulation of native microorganisms for biocementation in samples recovered from field-scale treatment depths. J Geotech Geoenviron Eng 144(1):04017098. https://doi.org/10.1061/(ASCE)GT.1943-5606.0001804

Gurevich A, Saveliev V, Vyahhi N, Tesler G (2013) QUAST: quality assessment tool for genome assemblies. Bioinformatics 29:1072–1075

Hu Y, Liu W, Wang W, Jia X, Xu L, Cao Q, Shen J, Hu X (2020) Biomineralization performance of Bacillus sphaericus under the action of Bacillus mucilaginosus https://doi.org/10.1155/2020/6483803

Jaya P, Nathan VK, Ammini P (2019a) Characterisation of marine bacterial carbonic anhydrase and their CO_2 sequestration abilities based on a soil microcosm. Prep Biochem Biotechnol 49(9):891–899. https://doi.org/10.1080/10826068.2019.16336

Kichou Z, Mavroulidou M, Gunn MJ (2022) Investigation of the strength evolution of lime-treated London clay soil. Proceedings of the Institution of Civil Engineers-Ground Improvement https://doi.org/10.1680/jgrim.21.00053

Klier M, Andes FT, Deitmer JW, Becker HM (2014) Intracellular and extracellular carbonic anhydrases cooperate non-enzymatically to enhance the activity of monocarboxylate transporters. J Biol Chem 289(5):2765–2775

Jaya P, Nathan VK, Ammini P (2019b) Characterization of marine bacterial carbonic anhydrase and their CO_2 sequestration abilities based on a soil microcosm. Prep Biochem Biotechnol 49:891–899. https://doi.org/10.1080/10826068.2019.1633669

Lee MD (2019) GToTree: a user-friendly workflow for phylogenomics. Bioinforma Oxf Engl 35:4162–4164

Lee M, Gomez MG Graddy CMR et al (2023) Improving the spatial control of soil biocementation using indigenous microorganisms: column experiments and reactive transport modeling Engineering Geology 318 (2023) 107104 https://doi.org/10.1016/j.enggeo.2023.107104

Lorenzo GA, Bergado DT (2006) Fundamental characteristics of cement-admixed clay in deep mixing. J Mater Civ Eng 18(2):161–174

Martin V et al (2009) Recombinant plant gamma carbonic anhydrase homotrimers bind inorganic carbon. FEBS Lett 583:3425–3430. https://doi.org/10.1016/j.febslet.2009.09.055

Mavroulidou M et al (2023) An assessment of different alkali-activated cements as stabilisers of sulphate-bearing soils. Q J Eng Geol Hydrogeol. https://doi.org/10.1144/qjegh2022-057

Mavroulidou M, Feruku B, Boulouki G (2022a) Properties of structural concrete with high-strength cement mixes containing waste paper sludge ash. J Mater Cycles Waste Manage 24:1317–1332. https://doi.org/10.1007/s10163-022-01402-z

Mavroulidou M et al (2022b) A Study of Innovative Alkali-Activated Binders for Soil Stabilisation in the Context of Engineering Sustainability and Circular Economy. Circular Econ Sustain 2:1627–1651. https://doi.org/10.1007/s43615-021-00112-2

Muley P, Dhumal M, Vora D (2014) Sequestration of atmospheric carbon dioxide by microbial carbonic anhydrase. IOSR. J Environ Sci Toxicol Food Technol 8:45–48

Mwandira W et al (2019) Efficacy of biocementation of lead mine waste from the Kabwe Mine site evaluated using Pararhodobacter sp. Environ Sci Pollut Res 26:15653–15664. https://doi.org/10.1007/s11356-019-04984-8

Mwandira W et al (2021) Solidification of sand by Pb (II)-tolerant bacteria for capping mine waste to control metallic dust: case of the abandoned Kabwe Mine Zambia. Chemosphere 228:17–25. https://doi.org/10.1016/j.chemosphere.2019.04.107

Mwandira W., et al (2023a) An electrokinetic-biocementation study for clay stabilisation using carbonic anhydrase-producing bacteria. Environ Sci Pollut Res, 30, 104916–104931 https://doi.org/10.1007/s11356-023-29817-7

Mwandira W et al (2023b) Concurrent carbon capture and biocementation through the carbonic anhydrase (CA) activity of microorganisms-a review and outlook. Environ Process 10(4):56. https://doi.org/10.1007/s40710-023-00667-2

Mwandira W et al (2023c) Synthesis and utilisation of hybrid metal-carbonic anhydrase enzyme carrier system for soil biocementation. Appl Sci 13(17):9494. https://doi.org/10.3390/app13179494

Mwandira W. et al, (2023d) Biocementation mediated by native carbonic anhydrase-producing microbes. In. Proceedings of the Tenth International Conference on Environmental Management, Engineering, Planning & Economics Skiathos Island, Greece, June 5–9, 2023, 237–246, ISBN: 978–618–5710–25–5

Naeimi M, Haddad A (2020) Environmental impacts of chemical and microbial grouting. Environ Sci Pollut Res 27:2264–2272. https://doi.org/10.1007/s11356-019-06614-9

Nathan VK, Ammini P (2019) Carbon dioxide sequestering ability of bacterial carbonic anhydrase in a mangrove soil microcosm and its bio-mineralization properties. Water, Air, & Soil Pollution 230. https://doi.org/10.1007/s11270-019-4229-3

Parks DH et al (2015) CheckM: assessing the quality of microbial genomes recovered from isolates, single cells, and metagenomes. Genome Res 25:1043–1055

Peng Y, Leung HCM, Yiu SM, Chin FYL (2012) IDBA-UD: a de novo assembler for single-cell and metagenomic sequencing data with highly uneven depth. Bioinforma Oxf Engl 28:1420–1428

Porter H, Mukherjee A, Tuladhar R, Dhami NK (2021) Life cycle assessment of biocement: an emerging sustainable solution? Sustainability 13:13878. https://doi.org/10.3390/su132413878

Price MN, Dehal PS, Arkin AP (2010) FastTree 2 – approximately maximum-likelihood trees for large alignments. PLoS ONE 5:e9490

Rambaut, A. (2018) Releases rambaut/figtree. GitHub https://github.com/rambaut/figtree/releases

Rios S, Ramos C, Viana da Fonseca A, Cruz N, Rodrigues C (2019) Mechanical and durability properties of a soil stabilised with an alkali-activated cement. Eur J Environ Civ Eng 23:245–267

Safdar MU et al (2021a) Innovative methods of ground improvement for railway embankment peat fens foundation soil. Géotechnique 71(11):985–998. https://doi.org/10.1680/jgeot.19.SiP.030

Safdar MU et al (2021b) Electrokinetic biocementation of an organic soil. Sustain Chem Pharm 21:100405. https://doi.org/10.1016/j.scp.2021.100405

Safdar MU et al (2022) Towards the development of sustainable ground improvement techniques-biocementation study of an organic soil. Circular Econ Sustain https://doi.org/10.1007/s43615-021-00071-8

Shen , Xiong J (2019) TaxonKit: a cross-platform and efficient NCBI taxonomy toolkit. http://biorxiv.org/lookup/doi/10.1101/513523

Singhi B, Laskar AI, Ahmed MA (2017) Mechanical behavior and sulfate resistance of alkali activated stabilized clayey soil. Geotech Geol Eng 35(5):1907–1920

Tange O (2018) Gnu Parallel 2018. (Zenodo, 2018). https://doi.org/10.5281/ZENODO.1146014

Tatusova T et al (2016) NCBI prokaryotic genome annotation pipeline. Nucleic Acids Res. 2016 Aug 19;44(14):6614–24. https://doi.org/10.1093/nar/gkw569. Epub 2016 Jun 24. PMID: 27342282; PMCID: PMC5001611.

Tu C, Foster L, Alvarado A (2012) Role of zinc in catalytic activity of carbonic anhydrase IX. Arch Biochem Biophys 521(1–2):90–94. https://doi.org/10.1016/j.abb.2012.03.017

van Paassen LA et al (2010) Quantifying biomediated ground improvement by ureolysis: large-scale biogrout experiment. J Geotech Geoenviron Eng 136:1721–1728. https://doi.org/10.1061/(ASCE)GT.1943-5606.0000382

Vaughan A (2022) UK's largest carbon capture project will turn CO_2 into baking soda, New Scientist, 24 June 2022. Available from: https://www.newscientist.com/article/2325858-uks-largest-carbon-capture-project-will-turn-co2-into-baking-soda/ (accessed 30/10/2023)

Whiffin VS (2004) Microbial $CaCO_3$ precipitation for the production of biocement, PhD thesis, Murdoch University, Perth, Western Australia. (online) https://researchrepository.murdoch.edu.au/id/eprint/399/2/02Whole.pdf (accessed: 08/11/2023)

Zhang X, Mavroulidou M, Gunn MJ, Kichou Z (2014) Application of a novel laser sensor volume measurement system to the triaxial testing of an unsaturated lime-treated soil. Acta Geotech 9(6):945–957

Zhang X, Mavroulidou M, Gunn MJ (2015) Mechanical properties and behaviour of a partially saturated lime-treated, high plasticity clay. Eng Geol 193:320–336

Zheng T, Qian C (2020) Influencing factors and formation mechanism of $CaCO_3$ precipitation induced by microbial carbonic anhydrase. Process biochemistry (1991) 91:271-281 https://doi.org/10.1016/j.procbio.2019.12.018